Indian J Phys **44**, 188–193 (1970)

Modular spark chamber

SAMIR GHOSH*, J. P. MUNDRA AND D. MAJUMDAR

Physical Laboratory, Presidency College, Calcutta

(*Received* 9 *February* 1970)

(Plates—7)

In this paper the construction and operation of three different types of spark chambers are described In particular, the operations of the modular spark chamber with argon and neon fillings at various pressures lower than one atmosphere are analysed.

INTRODUCTION

During the last few years spark chambers have been developed with subsequent sophistications as a detector of charged particles. Spark chambers have the unique property of simplicity of operation coupled with the visual manifestation of the path of the charged particles In this laboratory, so long the charged particles were studied with the help of Wilson's cloud chamber and neon tube hodoscope. Now a modular spark chamber has been developed, experimenting from the primary stage This spark chamber has the special feature of simplicity of construction and of operation.

SPARK CHAMBERS

Before this modular spark chamber was developed, two other spark chambers were made in our laboratory with different variable spark gaps and thicknesses of the electrodes. The spark chambers can be constructed without the help of any sophisticated mechanical workshop.

The electrodes of the first spark chamber were made of aluminium sheets of thickness 0·3 mm and individual electrodes were kept apart from one another with the help of perspex spacers. The spark gaps of this 4-gap spark chamber were 5·0 mm and the sensitive area was 117 sq cm. Each pair of two electrodes of same potential were placed facing each other and were kept insulated from each other to facilitate the application of different potentials at different spark gaps and also for connecting different condenser banks to different spark gaps

The primary difficulty in constructing a spark chamber arises from extraneous sparking at the edges of the electrodes at relatively lower voltages because of sharpness and consequent production of high electric fields at the edges of the electrodes. This difficulty was circumvented by turning the edges of the electrodes in the form of spirals; the spirals being away from the electrodes with opposite potentials (figure 1, plates 7).

* Present address : Department of Radiotherapy, Medical College Hospitals, Cal.-12.

Out of the four sharp edges of the aluminium electrodes the extraneous sparking at two edges, parallel to the axis of the camera, were avoided by this method and the extraneous sparking at voltages, relatively lower than the operating voltage, at two other edges, perpendicular to the axis of the camera, were avoided by placing the electrodes of opposite potentials in criss-cross manner and thereby increasing the distances between the edges. The electrodes were of rectangular shape and the broad-sides of the earthed electrodes were placed facing the long-sides of the high-potential electrodes. In figure 1 (plates 7) this arrangement has been shown. The reflection from the glazing aluminium surfaces was avoided by painting the surfaces with a conducting black paint, taking care that no sharp point is formed thereby. The schematic diagram in figure 2 shows the dimensions of the spark chamber.

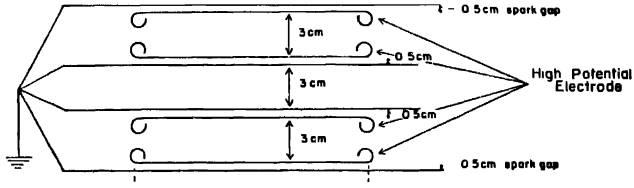

FRONT VIEW

FIGURE 2. The Schematic diagram of Spark Chamber—Model 1.

The whole assembly of this 4-gap spark chamber was placed within an air-tight perspex box, the electrical feedthrough being sealed at the sides of the box. Two nozzles were fitted at two opposite corners of the box for the inlet and outlet of gases. The photography was done from ouside this transparent box.

The spark chamber was run first with air inside it and next the air was completely flushed out with argon through the inlet, keeping the outlet open during replacement, and the spark chamber was closed, with argon at atmospheric pressure.

The variations of the threshold voltage (*i.e.*, where the spark appears only in case of passage of heavily ionizing particles) and the breakdown voltage (*i.e.* where the sparking takes place even without the passage of ionizing particles through the sensitive area of the chamber) due to the nature of the gas within the chamber have been studied and the results are given in table 1. The working voltage lies in between threshold and working voltages.

To study the effect of clearing field, potentials of the order of 45 volts and 90 volts were applied in between each pair of opposite electrodes and in opposition to the high-voltage pulses from a 5C22 hydrogen thyratron. The results of these experiments are also incorporated in table 1.

Table 1

(Spark gap = 5.0 mm)

Gas in chamber	Clearing field, volts	Threshold voltage, kV	Breakdown voltage, kV
Air	0	8.9	9.3
	45	9 1	9.6
	90	9 1	9.6
Argon	0	8.2	8.7
	45	8.2	8.9
	90	8.2	8.9

Table 1 shows that the doubling of the clearing field from 45 V to 90 V has no effect either on the threshold or on the breakdown voltages.

To facilitate the variations of spark gaps and for shortening the space lost due to the spiral formations of the electrodes at the edges, the second spark chamber (Model 2) was constructed with a different design. The electrodes, as before, were made of aluminium and were of thickness 0·55 mm. The sensitive area of the chamber was 175·5 sq cm. The perspex spacers were replaced with glass spacers in the form of tubes and rods. By punching holes at the four corners of the electrodes, these were slided down the glass rods fixed at four corners of the base plate and the spacings in between the electrodes were maintained by sliding glass tubes down the glass rods. The spark gaps could easily be varied by changing the lengths of these glass tubes. The spiral form at the edges of the electrodes was changed to an U-shaped bend with the ends bent inwards (figure 3—plate 7).

In this case also the whole assembly was placed within an air-tight perspex box and experiments performed by filling the chamber with air and argon. The results of these experiments are given in table 2. The effects of varying the clearing field are also shown in this table. These results are for the corresponding spark gap of 3·0 mm.

The gaps in between the electrodes of same potential can be properly utilized for placing in required absorbers for different experiments.

Table 2

(Spark gap = 3,0 mm)

Gas in chamber	Clearing field, volts	Threshold voltage, kV	Breakdown voltage, kV
	0	5.7	6.4
	45	6 1	6.4
argon	0	5.0	5.9
	45	5.3	6.1

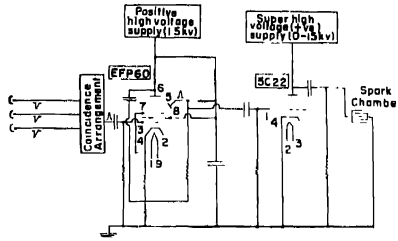

FIGURE 4 Schematic Diagram of the circuit.

Both the above two spark chambers were triggered by charged particles collimated by three GM-counters. The schematic diagram in figure 4 shows the circuit used for the operation of these spark chambers. The coincidence pulses from three GM-counters were fed into the grid of an EFP60 tube giving rise to a 400 V positive pulse at the cathode of the EFP60 and these high-voltage pulses were fed in their turn into the grid of the 5C22 hydrogen thyratron operating at potentials upto 15 kV. The super-high voltage pulses from the hydrogen thyratron were communicated to the high potential electrodes of the spark chambers.

MODULAR SPARK CHAMBER

In the next phase of development we have made a 4-gap modular spark chamber of spark gaps 12·4 mm. To avoid the non-uniformity of spark gaps due to the sagging in case of very thin electrodes, we have used aluminium plates of thickness 1·4 mm for intermediate electrodes and the two end electrodes were made out of thicker aluminium plates of thickness 3·4 mm. The end electrodes were made out of thicker plates since these are to withstand the atmospheric pressure when the chamber is evacuated with a vacuum pump to fill it up with argon or neon The aluminium plates were glued to either sides of perspex frames, made by grooving out the central region from perspex sheets of thickness 12·4 mm The edges of the electrodes were kept protruding outside in air (figure 5—plate 7).

When the spark chamber is filled with argon or neon the extremities of the electrodes remain in air and since in case of argon or neon the working voltages are much lower than the corresponding working voltages for air for a particular spark gap, there is no possibility of edge effects.

The individual compartments of the 4-gap spark hamber were interconnected by making small holes in the intermediate electrodes. Since making of holes can give rise to effect, similar to edge effect, because of sharpness around the edges of the holes, the holes were made funnel shaped (figure 6). A glass nozzle was sealed through the side of the last compartment to draw out the air and to fill it up subsequently with argon or neon.

FIGURE 6. Interconnection between chamber gaps.

The same triggering arrangement and operating circuits which have been used in case of operation of the first two spark chambers have also been utilized for the operation of this modular spark chamber. The tracks of charged particles (μ-mesons) recorded by this chamber are sufficiently sharp for analysis. Since, as triggering particle collimated cosmic-ray beam has been used, the resolution of the chamber has not been needed to be improved with the help of clearing field.

PRESSURE—VOLTAGE RELATION

The dependence of optimum working voltage on pressure of argon within the spark chamber has been studied and the results are shown by the corresponding curve in figure 7.

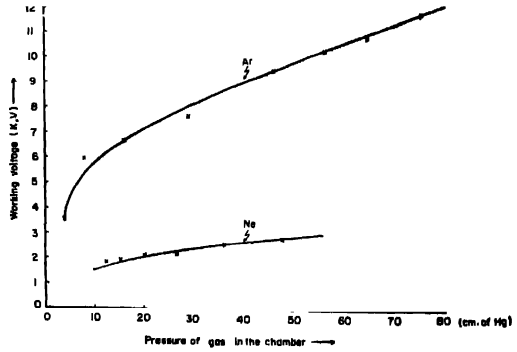

FIGURE 7. Working voltage dependence on Prossure of gas in the chamber.

Indian J. Phys. Volume **44**, *No. 3, 1970*
PLATE 7

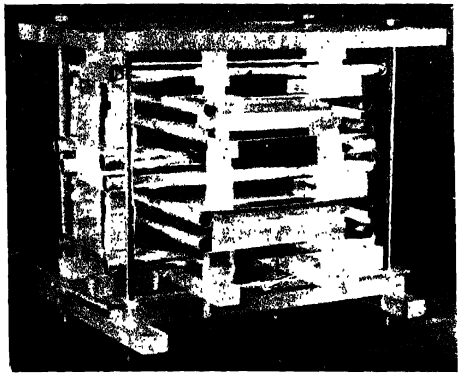

Figure 1. Spark chamber—Model 1.

Figure 3 Spark chamber—Model 2

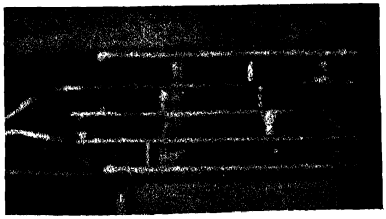

Figure 5 Modular spark chamber

It is observed that in the range of 10 cm to 75 cm of Hg pressure the curve follows the following quadratic equation :—

$$Y = 3{\cdot}76 + 1{\cdot}59 \times 10^{-1}\, X - 7{\cdot}7 \times 10^{-4}\, X^2 \qquad \ldots (1)$$

At lower pressure, about 4 cm of Hg the sparking phenomenon changed into the low pressure discharge phenomenon. It shows that the minimum pressure for the working of the argon-filled spark chamber lies in between 4 and 10 cm of Hg pressure. The construction of this particular modular spark chamber did not permit us to study the dependence of working voltage on pressures of argon higher than the atmospheric pressure. But there is no ground to expect the curve in figure 7 to deviate from its nature at pressures above one atmosphere.

The modular spark chamber was next filled up with pure neon and the dependence of optimum working voltage on pressure was studied and the results were plotted in the corresponding curve in figure 7 for neon. The curve for neon follows the following quadratic equation :—

$$Y' = 1{\cdot}542 + 3{\cdot}006 \times 10^{-2}\, X - 7{\cdot}845 \times 10^{-5}\, X^2 \qquad \ldots (2)$$

The curve for neon lies much below the corresponding curve for argon, showing that the working voltage required for neon-filled chambers are much lower than argon-filled chambers.

ACKNOWLEDGEMENT

The authors are grateful for the financial support given by the Government of West Bengal, India for this work. They offer sincere thanks to Prof. R. L. Sen Gupta and Prof. P. K. Sen Chaudhury for their interest and encouragement.

REFERENCES

Roy C, & Parker S. 1963, *Nuclear Instruments & Methods*, **20**, 173.